

1 **Quantifying the effects of switchgrass (*Panicum virgatum*) on deep organic C stocks**
2 **using natural abundance ^{14}C in three marginal soils**

3 Eric W. Slessarev^{1*}

4 Erin E. Nuccio¹

5 Karis J. McFarlane¹

6 Christina Ramon¹

7 Malay Saha²

8 Mary K. Firestone³

9 Jennifer Pett-Ridge^{1*}

10

11 ¹ Physical and Life Sciences Directorate, Lawrence Livermore National Laboratory, Livermore,
12 CA, USA

13 ² Noble Research Institute, Ardmore, OK, USA

14 ³ Environmental Science, Policy and Management Department, University of California,
15 Berkeley, Berkeley, CA, USA

16

17 *slessarev1@llnl.gov

18 *pettridge2@llnl.gov

19

20 Running head: Quantifying deep soil organic C under switchgrass

21 Key words: Switchgrass, Soil carbon, Marginal lands, Radiocarbon, Deep roots, Stable isotopes

22

23

24

25

26

27

28

29

30

31 **Abstract**

32 Perennial bioenergy crops have been shown to increase soil organic carbon (SOC) stocks,
33 potentially offsetting anthropogenic C emissions. The effects of perennial bioenergy crops on
34 SOC are typically assessed at shallow depths (< 30 cm), but the deep root systems of these crops
35 may also have substantial effects on SOC stocks at greater depths. We hypothesized that deep (>
36 30 cm) soil organic carbon (SOC) stocks would be greater under bioenergy crops relative to
37 stocks under shallow-rooted conventional crop cover. To test this, we sampled soils to between
38 1- and 3-meters depth at three sites in Oklahoma with 10-20 year old switchgrass (*Panicum*
39 *virgatum*) stands, and collected paired samples from nearby fields cultivated with shallow rooted
40 annual crops. We measured root biomass, total organic C, ¹⁴C, ¹³C, and other soil properties in
41 three replicate soil cores in each field and used a mixing model to estimate the proportion of
42 recently fixed C under switchgrass based on ¹⁴C. The subsoil C stock under switchgrass (defined
43 over 500-1500 kg m⁻² equivalent soil mass, approximately 30-100 cm depth) exceeded the
44 subsoil stock in neighboring fields by 1.5 kg C m⁻² at a sandy loam site, 0.6 kg C m⁻² at a site
45 with loam soils, and showed no significant difference at a third site with clay soils. Using the
46 mixing model, we estimated that additional SOC introduced after switchgrass cultivation
47 comprised 31% of the subsoil C stock at the sandy loam site, 22% at the loam site, and 0% at the
48 clay site. These results suggest that switchgrass can contribute significantly to subsoil organic
49 C—but also indicated that this effect varies across sites. Our analysis shows that agricultural
50 strategies that emphasize deep-rooted grass cultivars can increase soil C relative to conventional
51 crops while expanding energy biomass production on marginal lands.

52 **1. Introduction**

53 Soil horizons deeper than 30 cm contain the majority of Earth’s soil organic carbon (SOC)—
54 possibly holding well over 1000 Pg of C globally (Harrison et al., 2010; Jobbágy and Jackson,
55 2000). While the bulk of deep soil C tends to exchange slowly with the atmosphere (Mathieu et
56 al., 2015; Trumbore, 2009), SOC losses from deep soil horizons following land use change have
57 been substantial—accounting for the majority of the 133 Pg of SOC lost following the global
58 expansion of agriculture (Sanderman et al., 2017). By implication, successful attempts to reverse
59 SOC loss in agricultural lands must restore SOC in deep horizons. Furthermore, C concentrations
60 at depth are relatively low—implying that subsoils have a large capacity to store C and thus
61 might sequester a significant amount of additional atmospheric CO₂ (Lorenz and Lal, 2005;
62 Minasny et al., 2017; Paustian et al., 2016; Rumpel and Kögel-Knabner, 2011).

63 A range of processes introduce C to subsoils, including dissolved C transport in
64 percolating water, burial of aboveground litter via physical mixing, and C fluxes from root
65 exudates and root turnover at depth (Rumpel and Kögel-Knabner, 2011). Deep roots in particular
66 have been identified as a potentially useful conduit for increasing subsoil C stocks in managed
67 landscapes (Kell, 2012; Lynch and Wojciechowski, 2015). A large fraction of SOC is root
68 derived, and the depth distribution of SOC correlates with rooting distributions across biomes in
69 natural ecosystems (Grayston et al., 1997; Jobbágy and Jackson, 2000; Rasse et al., 2005). Dead
70 roots and root exudates fuel production of microbial biomass, which subsequently becomes a
71 primary source of mineral-associated C that can persist over long timescales (Sokol et al., 2019).
72 Deeply rooted bioenergy crops can also enhance production of microbial extracellular
73 polysaccharides, cementing soil aggregates that may protect SOC (Sher et al., 2020). In theory,
74 increasing SOC via deep roots might be achieved without displacing conventional food crops if
75 bioenergy crops are grown on marginal lands—which are otherwise not ideal for food production

76 due to low fertility or environmental sensitivity (Gelfand et al., 2013; Lemus and Lal, 2005;
77 Robertson et al., 2017).

78 While cultivation of perennial bioenergy crops and restoration of perennial grasslands
79 have been widely shown to increase SOC stocks relative to stocks under conventional crops, the
80 majority of studies have focused on the top 30 cm of soil (Anderson-Teixeira et al., 2009;
81 Beniston et al., 2014; Conant et al., 2017; Harris et al., 2015; Monti et al., 2012; Qin et al.,
82 2016). Furthermore, the magnitude of the difference in SOC stocks following conversion to
83 perennial grassland is highly variable (Conant et al., 2017). Predicting the effect of deep roots on
84 subsoil C across different soil types will ultimately require more field studies spanning edaphic
85 gradients that sample deeply (i.e. ≥ 1 m).

86 Evaluating the effects of deep roots on subsoil C in the field is challenging, however,
87 because differences in SOC stocks between different land use types are often small relative to
88 total SOC stocks (Syswerda et al., 2011). Ideally changes in SOC under different plant types
89 would be quantified in long-term experiments in which initial conditions are controlled and
90 quantified (Liebig et al., 2008; Sanford et al., 2012). An alternative is to sample opportunistically
91 using a paired design (Fisher et al., 1994; Liebig et al., 2005); in this case the plant cover of
92 interest is compared to a neighboring “reference field” representing the conventional
93 management practice and initial conditions are assumed to be the same across the two plots. This
94 approach cannot detect net change SOC over time given that SOC stocks in the reference plot
95 may not be at steady state—but it can detect divergence in SOC stocks under different
96 management scenarios (Sanderman and Baldock, 2010). Furthermore, the paired design can be
97 applied rapidly in locations where initial data are unavailable, enabling wider sampling of
98 edaphic gradients.

99 Naturally occurring C isotopes (^{13}C , ^{14}C) can be used as sensitive tracers of C fluxes
100 (Jones and Donnelly, 2004), and are useful for constraining the effect of deep roots on subsoil C
101 when the paired sampling approach is applied (Balesdent et al., 2018; Marin-Spiotta et al., 2009;
102 O'Brien et al., 2013; Richter et al., 1999). For instance, ^{13}C is commonly used to quantify the
103 fraction of SOC derived from recent plant inputs in cases where the photosynthetic pathway of
104 the plant cover is replaced, changing the ^{13}C signature of the inputs (Balesdent et al., 2018, 1987;
105 Garten and Wullschleger, 2000). However, ^{13}C -based mixing models require a clear transition
106 between C_3 and C_4 vegetation (Balesdent and Mariotti, 1996), and are thus challenging to apply
107 in agricultural systems with complex cropping histories.

108 In systems where no clear transition between C_3 and C_4 vegetation have occurred, the
109 radioisotope ^{14}C provides an alternative to ^{13}C . Atmospheric radiocarbon concentrations are
110 sustained by production of ^{14}C in the stratosphere, and were elevated by introduction of ^{14}C from
111 atomic weapons testing during the 1950's and 60's (Hua et al., 2013). Deep soil C exchanges
112 slowly with the atmosphere and thus becomes naturally depleted in ^{14}C as it undergoes
113 radioactive decay (Trumbore, 2009). Consequently, recently fixed C introduced to subsoils via
114 increased root production should have an elevated ^{14}C signature relative to the preexisting
115 subsoil C pool (Richter et al., 1999). ^{14}C can thus provide upper limits on the magnitude of
116 differences in SOC that emerge after replacing conventional crops with deeply rooted crops.

117 In this paper, we explore C storage in marginal lands cultivated with switchgrass (*Panicum*
118 *virgatum*, L.), a deeply rooted perennial grass grown as forage and as a cellulosic bioenergy
119 feedstock. We used a paired sampling design at three sites in Oklahoma with different soil
120 textures that experienced soil degradation during the American Dust Bowl and were planted with
121 switchgrass in either 1998 or 2008 and sampled in 2018. Given that 10 years is typically
122 sufficient to measure C stock differences at shallow depths (< 30 cm) when comparing

123 switchgrass to conventional cropland (Anderson-Teixeira et al., 2009), we hypothesized that C
124 stocks at greater depths (> 30 cm) would also diverge between switchgrass and paired reference
125 plots over this timespan. Identifying rates of SOC divergence in subsoils under perennial
126 bioenergy crops is important because the majority of existing studies on land conversion to
127 perennial crops still deal with relatively shallow sampling depths: increasing the number of
128 studies that sample deeply is an imperative for improving regional- to global-scale prediction of
129 perennial crop effects on SOC (Ledo et al., 2020). We tested our hypothesis by quantifying both
130 total C and ^{14}C , which we used to develop sensitive estimates of the component of the total C
131 stock that could be attributed to switchgrass.

132 **2. Materials and Methods**

133 *2.1 Field sites*

134 Sampling took place in 2018 at three sites in Oklahoma, USA. At each site, we sampled deep soil
135 cores in >10 year old switchgrass plots and compared these with paired cores collected from
136 nearby fields cultivated with annual crops. The two sites in Southern Oklahoma; Red River farm,
137 Burneyville (hereafter the “Sandy Loam” site; Lat: 33°53'20.52"N, Lon: 97°17'7.13"W) and
138 Pasture Demonstration Farm, Ardmore (hereafter the “Clay” site; Lat: 34°13'11.00"N, Lon:
139 97°12'36.96"W) had been planted with “Alamo” switchgrass in 2008. The location in Northern
140 Oklahoma, near Stillwater (hereafter the “Loam” site; Lat: 36°8'0.16"N, Lon: 97°6'15.42"W),
141 was planted with “Kanlow” switchgrass in 1998. At the Sandy Loam site, switchgrass was uncut,
142 whereas at the Clay and Loam sites switchgrass was mowed and harvested annually (Loam) or 1-
143 2 times annual (Clay). The switchgrass stands at each site were unfertilized, although the stands
144 at the Clay site were originally established as part of a short-term P response study and thus
145 received fertilizer initially after planting. All three sites were near the outer geographic boundary

146 of the American Dust Bowl during the 1930s and likely experienced wind erosion at that time.
147 Before European settlement, the region likely hosted tall-grass prairie dominated by C₄ grasses
148 (Cotton et al., 2016). After European settlement in the 19th century, soils in the region were
149 cultivated with C₃ cereal crops (Paulsen and Shroyer, 2008). The three sites have a broadly
150 similar mean annual climate (Table 1).

151

Site	Latitude	Longitude	MAT (°C)	MAP (mm)
Sandy loam	33°53'20.52"N	97°17'7.13"W	17	954
Loam	36°8'0.16"N	97°6'15.42"W	16	933
Clay	34°13'11.00"N	97°12'36.96"W	17	959

152 **Table 1.** Location and climate of study sites. Mean annual temperature (MAT) and mean annual
153 precipitation (MAP) were obtained using gridded PRISM climate data (Prism Climate Group,
154 Oregon State University, 2011).

155

156 At the Sandy Loam site, the reference field had been cultivated with the C₃ grass rye
157 (*Secale cereal, L.*) in winter and the C₄ plant crabgrass [*Digitaria sanguinalis, (L.) Scop.*] in the
158 summer for at least the last 15 years under no-till management. Nitrogen fertilizer was applied at
159 approximately 150 kg N ha⁻¹ in the reference field annually at this site. At the Clay site, the most
160 recent species grown in the paired reference plots was wheat (*Triticum aestivum, L.*) with a
161 winter cover crop mix; this site was managed with conventional tillage, N was applied at an
162 average rate of 67 kg N ha⁻¹ annually, and fields were grazed by cattle in winter. At the Loam
163 site, the reference field was typically planted with wheat and managed with conventional
164 tillage—although during several years throughout 1998-2018 the reference field was planted

165 with the C₄ grass sorghum [*Sorghum bicolor*, (L.) Moench]; N was applied at an average rate of
166 72 kg ha⁻¹ annually. To our knowledge none of the sites were limed.

167 The sites spanned a soil texture gradient driven by parent material composition. The
168 Sandy Loam site featured coarse alluvial soils (Coarse-loamy, mixed, superactive, thermic Udic
169 Haplustolls) (National Cooperative Soil Survey, 2020). The Loam site featured soils derived
170 from alluvial and eolian deposits (Fine-loamy, mixed, superactive, thermic Fluventic
171 Haplustolls) (National Cooperative Soil Survey, 2020). Notably, the soils at this site included a
172 buried soil (paleosol) at > 1 m depth. The Clay site included a range of relatively fine-textured
173 soils weathered from Permian shales and sandstones (Fine-loamy, mixed, active, thermic Udic
174 Argiustolls) (National Cooperative Soil Survey, 2020). Soils at the third site varied between
175 clays, clay loams, and sandy clay loams based on the USDA texture classification system; we
176 chose the label “Clay” for this site because it was the most common texture class.

177 *2.2 Field sampling*

178 At each site, three soil cores were collected under switchgrass and three cores were
179 collected in an adjacent reference field. We treated the three cores taken in each field as replicate
180 samples, but we acknowledge that these cores are “pseudo-replicated” in that they were collected
181 from the same field, and that a larger sample size would have been ideal (Kravchenko and
182 Robertson, 2011). The low sample size was necessitated by the larger amount of labor required
183 to process > 3 m soil cores and the costs of radiocarbon analyses. Cores were spaced apart in
184 each field so that they would capture within-field variation to the extent possible: cores at the
185 Sandy Loam and the Clay sites were collected in June 2018, from a 20 m² area within each field,
186 and at the Loam site cores were collected Oct 1, 2018, also within a 20 m² area. The reference
187 fields at the Clay and Loam sites were approximately 50 m distant from the switchgrass fields,

188 and the reference field at the Sandy Loam site was approximately 500 m distant but situated in
189 the same soil series. Cores at the Sandy Loam and Cores were taken using a Giddings probe with
190 10.16 cm (4 inch) inner-diameter tooling and sampling 120 cm intervals. Sampling proceeded to
191 a depth of 3 m unless the probe reached refusal at a shallower depth (this occurred at the Clay
192 site at a depth of 120-150 cm, likely due to calcium cementation at depth). Each core was
193 photographed and divided into 30 cm intervals in the field. The reference plots were chosen to
194 match the soil properties of the switchgrass plots based on field observations.

195 At all sites, bulk density was estimated by weighing a 4 cm subsample from the center of
196 each core interval in the field and correcting for the gravimetric water content of the subsample
197 to obtain the subsample dry mass. This mass was then divided by the volume of the subsample to
198 calculate bulk density for that interval. Compression during sampling was on-average $7 \pm 5\%$ at
199 the Clay site and $< 1\%$ at the Loam and Sandy Loam sites. To account for compression during
200 sampling, volumes were linearly corrected over each sampling interval by scaling the observed
201 core length to the expected length (Parfitt et al., 2010). Particles > 2 mm comprised a negligible
202 fraction of the total mass of each interval, and so no correction for rock fraction was performed.
203 C stock calculations were later performed on an equivalent mineral soil mass basis to minimize
204 sensitivity to bulk density estimates (see below).

205 Roots were removed from the bulk density subsample by hand; approximately 20 person-
206 minutes were spent removing roots per interval. Roots were washed and dried to obtain the root
207 mass in each interval and scaled by the volume of the interval to obtain root biomass estimates.
208 Soil used for total C and C-isotope analysis was sampled from the remainder of the core interval
209 after removing 1 cm from its exterior to exclude soil from upper horizons that might have

210 contaminated the interval during sampling. Soil sampled from the interior of the core was sieved
211 to 2 mm and dried at 105 °C before being subdivided for physical and chemical analysis.

212 *2.3 Laboratory analyses*

213 Soil physical and chemical analyses were conducted at the Oregon State University Crop
214 and Soil Science Central Analytical laboratory (<https://cropandsoil.oregonstate.edu/cal>). Total C
215 and N were quantified by combustion at 1150 °C using an Elementar Macrocube analyzer. Soil
216 texture analysis, soil pH, and exchangeable cations were also quantified on samples from the 0-
217 30, 30-60, and 60-90 cm depth intervals and select intervals at greater depths. Texture was
218 quantified by the sieve and pipette method after removal of organic matter and carbonates (Burt,
219 2014). Soil pH was measured by electrode in a 1:1 soil:water slurry. Exchangeable cations were
220 quantified by 0.1 M barium chloride extraction and analysis by ICP-OES (Burt, 2014).

221 Inorganic C was quantified at Lawrence Livermore National Laboratory by treating finely-
222 ground subsamples of each sample with 1 M phosphoric acid in a sealed jar and measuring CO₂
223 evolved using a LI-850 infrared gas analyzer (Robertson, 1999). Where carbonates were present,
224 total organic C was obtained by subtracting inorganic C from total C.

225 C isotopes were quantified on a subset of the soil that was ground to a fine power by hand.
226 Soils that contained carbonates were treated with 1 M HCl to remove inorganic C before isotope
227 analysis. Direct addition of dilute (~ 1 M) HCl has measurable but relatively small (< 1‰)
228 effects on ¹³C and ¹⁴C in soils and sediments (Brodie et al., 2011; Komada et al., 2008) and
229 appears to be no more biased than alternative treatment approaches (Brodie et al., 2011). HCl
230 was added to each sample until effervescence ceased and then was allowed to evaporate to
231 prevent leaching of acid-soluble C. Acid-treated soil was analyzed for ¹³C at the University of
232 California Berkeley Center for Stable Isotope Biogeochemistry

233 (<https://nature.berkeley.edu/stableisotopelab/>). The ^{13}C content of each sample ($\delta^{13}\text{C}$) was
234 reported in per mil (‰) relative to the V-PDB isotope standard. Radiocarbon values were
235 measured on the NEC 1.0 MV Tandem accelerator mass spectrometer (AMS) or the FN Tandem
236 Van de Graaff AMS at the Center for AMS at Lawrence Livermore National Laboratory.
237 Samples were prepared for ^{14}C measurement by sealed-tube combustion to CO_2 in the presence
238 of CuO and Ag and then reduced onto iron powder in the presence of H_2 (Vogel et al., 1984).
239 The ^{14}C content of each sample ($\Delta^{14}\text{C}$) was reported in ‰ relative to the absolute atmospheric
240 ^{14}C activity in 1950. We report $\Delta^{14}\text{C}$ here rather than mean residence times because reporting
241 $\Delta^{14}\text{C}$ does not require an assumption that SOC pools are at equilibrium; negative $\Delta^{14}\text{C}$ values
242 generally indicate less interaction between SOC and the atmosphere and longer SOC residence
243 times. To calculate $\Delta^{14}\text{C}$, measured $\delta^{13}\text{C}$ values were used to correct for mass dependent
244 fractionation to yield ^{14}C activity at a reference $\delta^{13}\text{C}$ of -25‰ (Stuiver and Polach, 1977).
245 Radiocarbon analyses were conducted in late 2018 – 2019 (exact dates are listed for each sample
246 in Supplementary Table 1). Because collection and analysis occurred within a short period, no
247 correction was performed for decay of ^{14}C between sampling and analysis. The average
248 instrument uncertainty for $\Delta^{14}\text{C}$ was ± 4 ‰, and the average precision estimated from a set of six
249 duplicate samples was ± 5 ‰.

250 *2.4 C stock calculations*

251 We used measured C stocks to directly estimate the net difference in C between the
252 switchgrass and reference fields. We also used ^{14}C measurements to develop an indirect estimate
253 that was independent of the measured C stock in the reference field. The C stock calculations
254 were carried out on an equivalent soil mass (ESM) basis using the cumulative coordinate
255 approach (Gifford and Roderick, 2003; Rovira et al., 2015). We used this approach because it is

256 robust to differences in bulk density, and thus better suited to comparing C stocks under different
257 land uses (Wendt and Hauser, 2013). Calculations were performed separately on the surface soil
258 layers—which we defined as the top 500 kg m⁻² of soil—and the subsoil—which we defined as
259 the 1000 kg m⁻² of soil directly below the uppermost 500 kg m⁻² of soil.

260 We obtained C stocks by using linear interpolation to predict cumulative C mass from
261 cumulative soil mass (Gifford and Roderick, 2003). The mineral mass of each depth interval was
262 used as the basis for developing mass coordinates (Rovira et al., 2015). Mineral mass was
263 obtained by multiplying the mass of the interval by the 1 minus the soil organic matter fraction
264 [soil organic matter fraction = % organic carbon * (1/100) *2; (Pribyl, 2010)]. We then used
265 linear interpolation to develop a piece-wise function defining cumulative OC mass as a function
266 of cumulative mineral soil mass (Gifford and Roderick, 2003):

267 Equation 1:
$$C(t) = C(z_a) + \frac{C(z_b) - C(z_a)}{M(z_b) - M(z_a)} (M(t) - M(z_a))$$

268 Where C(t) is the cumulative C mass at the target cumulative soil mass M(t), C(z_a), and C(z_b) are
269 the cumulative C masses at the upper and lower a boundaries of the sampling interval containing
270 M(t), and M(z_a) and M(z_b) are the cumulative mineral masses at those boundaries (Gifford and
271 Roderick, 2003). Using this approach we estimated topsoil C contained in the first 500 kg m⁻² of
272 soil, and then obtained subsoil C by calculating the total C stock to 1500 kg m⁻² and subtracting
273 the topsoil C stock. Isotopic values for the topsoil and subsoil were calculated by weighting the
274 values associated with each sampling layer by the contribution of that layer to the C stock. When
275 the lower boundary of the topsoil or subsoil occurred within a layer, isotopic values from that
276 layer were weighted by the C mass that contributed to the topsoil or subsoil.

277 *2.5 Isotope calculations*

278 We initially explored the use of ^{13}C as a quantitative tracer of switchgrass inputs in our
279 system. The mixed history of C_3 and C_4 vegetation at all three sites—and in particular the recent
280 history of periodic C_4 cropping at the Sandy Loam and Loam sites—suggested that our sites did
281 not experience a clear transition between vegetation types. Depth weighted average $\delta^{13}\text{C}$ values
282 for the subsoil (defined over 500-1500 kg m^{-2} ESM) in the reference plots at our sites ranged
283 between 16.1 and -14.9 ‰, which is at the higher end of the C_4 plant range (O’Leary, 1988). We
284 measured the $\delta^{13}\text{C}$ of switchgrass roots at the three sites and obtained a range of -13.73 to -13.34
285 ‰—indicating that the difference between isotopic end-members in a potential ^{13}C -based mixing
286 model in the subsoil was only 2-3 ‰. This range is comparable to ~2 ‰ fractionation effects that
287 apply to plant-tissue end members in isotopic mixing models and are a possible source of
288 uncertainty (Menichetti et al., 2015; Werth and Kuzyakov, 2010). Given these clear limitations,
289 we concluded that $\delta^{13}\text{C}$ —while useful for qualitative interpretation of the SOC depth profiles at
290 our sites—could not be used for identifying switchgrass contributions to SOC quantitatively.

291 Instead of ^{13}C , we used ^{14}C to develop estimates of the amount of C introduced to
292 subsoils by switchgrass that were independent of the observed C stocks in the reference plots.
293 The ^{14}C signature of plant inputs depends on the composition of the atmosphere, and is thus
294 identical in switchgrass and reference plots. Consequently—while root derived inputs are
295 presumably lower under the reference vegetation—some atmospheric ^{14}C is introduced into the
296 subsoil in both cases, and ^{14}C can be used to identify net differences in C when comparing the
297 two plots. This contrasts with ^{13}C , which is typically used to estimate gross contributions of
298 recently fixed C in the context of paired sampling (Balesdent and Mariotti, 1996).

299 We did not carry out ^{14}C based calculations for the uppermost 500 kg m^{-2} of soil
300 (approximately 30 cm depth) because the $\Delta^{14}\text{C}$ values of the uppermost 500 kg of soil in the
301 reference plots were similar to the range of $\Delta^{14}\text{C}$ value of the recent atmosphere at two of the
302 sites. Specifically, we obtained empirical 95% confidence intervals for the $\Delta^{14}\text{C}$ value of the
303 uppermost 500 kg of soil using Monte-Carlo sampling (see Methods section 2.6 below) spanning
304 $[-74, 14] \text{ ‰}$ at the loam site and $[-160, -11] \text{ ‰}$ at the Sandy Loam site. These intervals
305 approached or overlapped the $\Delta^{14}\text{C}$ of the recent atmosphere [assumed to be -7 ‰ in 2018 (Hua
306 et al., 2013)], indicating little separation between the isotopic end-members at the surface. This
307 suggests that ^{14}C may only be a useful tracer of increased root inputs at depth, where SOC tends
308 to be ^{14}C depleted and contrasts strongly with recent inputs.

309 We divided the subsoil SOC stock under switchgrass (C_s , kg C m^{-2}) into two parts: (1) a
310 component equal to the C stock under the reference plot (C_r , kg C m^{-2}), representing the initial C
311 stock plus the mass of C equal to what was accrued or lost under the reference vegetation since
312 1998 or 2008; and (2) a component equal to the additional or “new” C accrued under switchgrass
313 since 1998 or 2008 (C_n , kg C m^{-2}). By definition $C_s = C_r + C_n$. Each of these components was
314 assigned an accompanying ^{14}C signature: Δ_r and Δ_s , which represented the measured $\Delta^{14}\text{C}$ of the
315 reference and switchgrass plot soils respectively, and Δ_n , which represented the assumed $\Delta^{14}\text{C}$ of
316 C_n . These values were related via an isotopic mixing equation:

317 Equation 2. $\Delta_s * C_s = \Delta_r * C_r + \Delta_n * C_n$

318 This mixing relationship was used to obtain the fraction (f_n) of the C stock under switchgrass
319 comprised by C_n and to solve for C_n :

320 Equation 3. $f_n = (\Delta_s - \Delta_r) / (\Delta_n - \Delta_r)$

321 Equation 4. $C_n = f_n * C_s \approx C_s - C_r$

322 The ^{14}C -based isotopic mixing model thus provided an estimate of the C stock difference based
323 on the observed C stock in the switchgrass plot and the shift in ^{14}C values between the two plots.

324 Parameterizing Equation 3 required three $\Delta^{14}\text{C}$ values: Δ_s , Δ_r , and Δ_n . We estimated Δ_s
325 and Δ_r as the stock-weighted average $\Delta^{14}\text{C}$ values of the subsoils in the switchgrass and reference
326 fields respectively. In contrast, Δ_n could not be assigned a fixed value because the $\Delta^{14}\text{C}$ of the
327 atmosphere changes over time and there can be lags between root production and integration of
328 root-C into SOC. However, Δ_n could be constrained within relatively narrow range based on the
329 known atmospheric $\Delta^{14}\text{C}$ and plausible decomposition rates for root-derived SOC since planting.
330 To constrain this range, we modeled the $\Delta^{14}\text{C}$ of SOC produced since 1998 or 2008 using a one-
331 pool soil C model.

332 The one-pool C model was implemented in SoilR (Sierra et al., 2012) using the function
333 “OnepModel14” and a published atmospheric CO_2 record for northern hemisphere, extended to
334 2018 by assuming a 5 ‰ annual decrease in atmospheric $\Delta^{14}\text{C}$ (Hua et al., 2013). The model was
335 initiated in 1998 or 2008 with zero initial C. Inputs were fixed at an arbitrary, constant, nonzero
336 value as the modeled $\Delta^{14}\text{C}$ value was independent of the input rate. While a varying input rate
337 would influence the modeled $\Delta^{14}\text{C}$ value of the SOC, we had no basis for parametrizing a
338 varying rate and the effect of varying inputs was small (e.g. halving litter inputs for the first four
339 years reduced the final $\Delta^{14}\text{C}$ by 4 ‰). The decomposition rate constant was set to two extreme
340 scenarios: either zero (no decomposition) or $\ln(2)$ (a one-year half-life). The modelled $\Delta^{14}\text{C}$
341 value of the SOC pool in 2018 under each scenario was used to define a range for Δ_n . This range
342 spanned from 0 ‰ to +15 ‰ for the Sandy Loam and Clay sites (planted in 2008), and from 0 ‰
343 to + 44 ‰ for the Loam site (planted in 1998).

344 2.6 Statistical analyses.

345 We evaluated C stock differences between the reference and switchgrass plots by
346 propagating statistical uncertainties using Monte Carlo simulations. Simulations were used to
347 obtain distributions for each estimate of the difference in C stocks between plots given the
348 uncertainties in the input parameters. We obtained 95% confidence intervals from the Monte
349 Carlo distribution of each estimate by computing quantiles of the final distributions (Buckland,
350 1984), and we obtained empirical p-values from the Monte Carlo intervals to test the hypothesis
351 that the difference in stocks was greater than zero. P-values were obtained using the formula $p =$
352 $(r + 1)/(n + 1)$, where r was the number of Monte Carlo replicates less than zero and n was the
353 total number of simulations (Davison and Hinkley, 1997). The error in each of the field-
354 measured properties (C stocks and isotope signatures) was modelled by generating normal
355 distributions with the standard deviation and mean obtained from the replicate cores (Huang,
356 2019). To generate the normal distributions, estimated standard deviations were corrected to
357 account for sample size by dividing them by a correction factor (c_4) which equals 0.886 when $n =$
358 3 (Huang, 2019). The distributions were assumed to vary independently. In the case of Δ_n , we
359 assumed a uniform distribution that ranged between the limiting cases defined in section 2.5
360 above. Parameter sets were drawn from the distributions 100,000 times. For each parameter set,
361 we calculated one of two quantities: an estimate of C_n from the observed stock difference ($C_s -$
362 C_r) or the ^{14}C -based stock difference ($f_n * C_s$).

363 3. Results

364 3.1 Soil physicochemical characteristics.

365 The three sites varied in texture, pH, and exchange properties (Table 2). Clay content and
366 exchangeable cation concentrations were lowest at the Sandy Loam site and highest at the Clay

367 site (Table 2). Ca was the dominant exchangeable cation at the Sandy Loam and Loam sites,
368 whereas Mg and Ca were approximately equal contributors at the Clay site (Table 2). Soil pH
369 values were mildly acid to mildly alkaline across three sites, and exchangeable Al concentrations
370 were below detection, or less than 1% of the total cation pool at all sites, and thus not reported.

371

372

Site	Particle size (%)			Exchangeable cations (meq 100g ⁻¹)				pH
	Sand	Silt	Clay	Ca	Mg	Na	K	
Sandy Loam	63 (3)	28 (3)	9 (1)	3.9 (0.5)	1.5 (0.2)	N.D	0.1 (0.04)	6.2 (0.2)
Loam	41 (6)	37 (5)	22 (2)	8.8 (0.8)	3.1 (0.4)	N.D	0.2 (0.03)	7.1 (0.5)
Clay	46 (10)	15 (7)	39 (13)	7.3 (1.4)	7.4 (4.0)	0.8 (1.0)	0.2 (0.02)	6.5 (0.4)

373

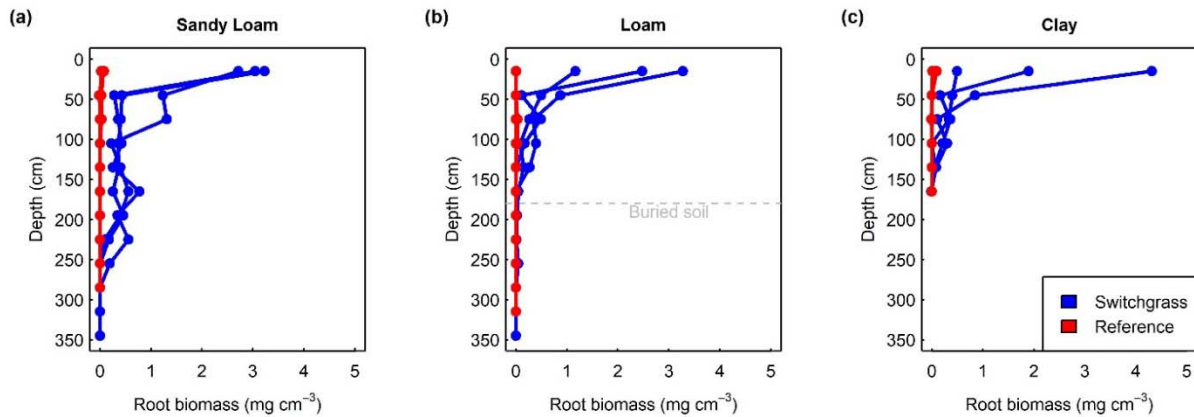
374 **Table 2.** Soil texture and exchange properties. Data are from three replicate cores sampled under
375 switchgrass and paired “reference” annual crops at three sites in Oklahoma characterized by
376 different soil textures. Values represent means of all six cores sampled at each site calculated on
377 averages of the top three depth intervals sampled (0-30, 30-60 and 60-90 cm). Standard
378 deviations are listed in parentheses.

379

380 *3.3 Root biomass*

381 Root biomass values and rooting depth under switchgrass differed substantially between
382 sites. Rooting profiles were deepest at the Sandy Loam site and comparatively shallower at the
383 Loam and Clay sites (Fig 1). Root biomass was much greater under switchgrass at all sites (Fig
384 1). However, the reference plots were sampled after harvest, and the small number of cores
385 collected (n = 3) may mean that we bypassed roots. Consequently these differences are likely not
386 representative of growing season conditions.

387



388

389 **Figure 1.** Root biomass versus depth. Data are from three replicate cores sampled under
390 switchgrass and paired “reference” annual crops at three sites in Oklahoma characterized by
391 different soil textures (Sandy Loam, panel a; Loam, panel b; Clay, panel c). Data from each
392 replicate core are shown individually. Cores taken under switchgrass are shown in blue, and
393 cores taken under the reference plot are shown in red. The soil at the Loam site (panel b) featured
394 a buried profile, which is shown with a dashed gray line.

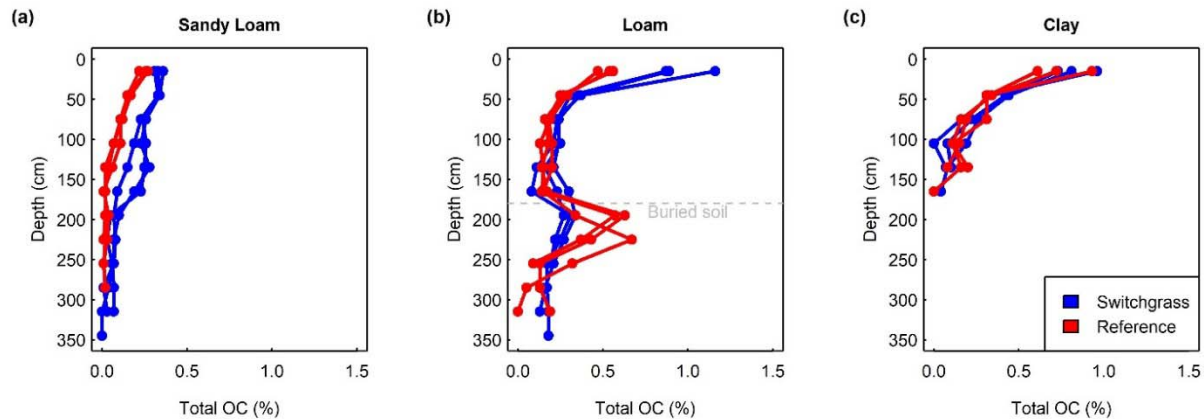
395

396 3.2 Organic C

397 Total organic C concentrations were lowest throughout the soil at the Sandy Loam site,
398 intermediate at the Loam site, and highest at the Clay site (Fig 2). At the Sandy Loam site,
399 organic C concentrations were highest in the three cores sampled under switchgrass throughout
400 the uppermost 200 cm of soil (Fig 2a). At the Loam site organic C concentrations were higher in
401 the cores sampled under switchgrass in the top 100 cm of the soil, with the largest difference in
402 the top 30 cm (Fig 2b). We also observed a substantial “bulge” in organic C below 200 cm at the
403 Loam site, which matched the top of the buried paleosol that we identified both in the soil series

404 description and in our field observations. The organic C content of the buried soil was higher in
405 the cores sampled under the reference vegetation (Fig 2b). In contrast to the Sandy Loam and
406 Loam sites, at the Clay site organic C concentrations were generally similar under both
407 vegetation types (Fig 2c).

408



409

410 **Figure 2.** Organic C concentrations versus depth. Data are from three replicate cores sampled
411 under switchgrass and paired “reference” annual crops at three sites in Oklahoma characterized
412 by different soil textures (Sandy Loam, panel a; Loam, panel b; Clay, panel c). Data from each
413 replicate core are shown individually. Cores taken under switchgrass are shown in blue, and
414 cores taken under the reference plot are shown in red. The soil at the Loam site (panel b) featured
415 a buried profile, which is shown with a dashed gray line.

416

417 3.4 Depth distribution of ^{13}C

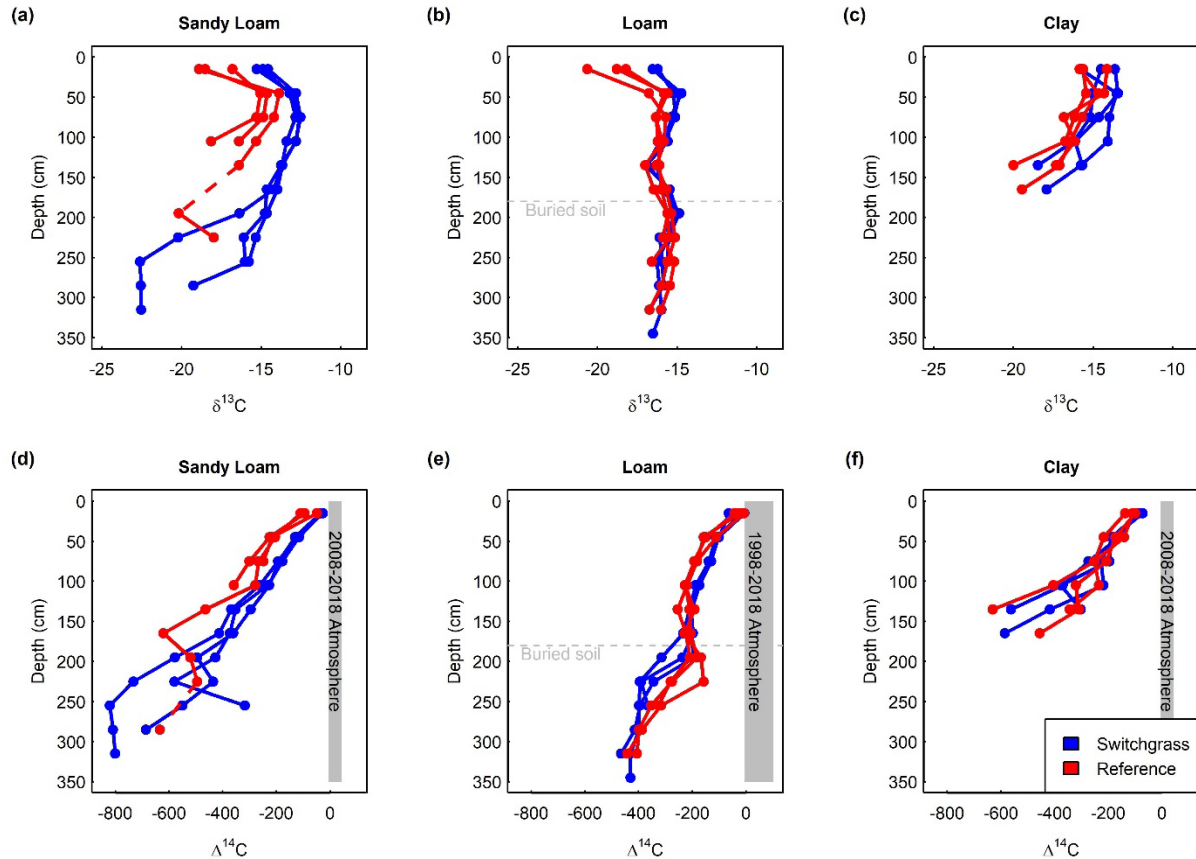
418 In general, the ^{13}C signature of organic C varied with sampling depth across sites. At the
419 Sandy Loam site, $\delta^{13}\text{C}$ values ranged from -20 to -16 ‰ in the top 30 cm of soil, increased by 3-
420 4 ‰ over 30-90 cm depth, and declined at greater depths (Fig 3a). This pattern appeared under

421 both plant types, but the $\delta^{13}\text{C}$ values were also approximately 2-3 ‰ higher under switchgrass
422 (Fig 3a). At the Loam site, $\delta^{13}\text{C}$ values were also depleted at the surface and comparatively
423 higher at greater depths in a pattern similar to the Sandy Loam site (Fig 3b). The $\delta^{13}\text{C}$ signature
424 was also comparatively higher in cores taken under switchgrass, but this difference attenuated
425 with depth (Fig 3b). At the Clay site, $\delta^{13}\text{C}$ values were highest at the surface and declined with
426 depth (Fig 3c). Patterns under the two plant covers at the Clay site were similar, with slightly
427 higher isotopic values under switchgrass (Fig 3c).

428 *3.5 Depth distribution of ^{14}C*

429 Radiocarbon values declined with depth at all sites (Fig 3d-f). At the Sandy Loam site
430 $\Delta^{14}\text{C}$ values were near zero at the surface and declined to values near -400 ‰ at 150 cm. Below
431 30 cm, $\Delta^{14}\text{C}$ values were systematically higher in cores taken under switchgrass (Fig 3d). At the
432 Loam site, $\Delta^{14}\text{C}$ values did not decline nearly as steeply as at the Sandy Loam site: at a depth of
433 150 cm $\Delta^{14}\text{C}$ was approximately 200 ‰. Between 30 and 90 cm the $\Delta^{14}\text{C}$ values of cores
434 sampled under switchgrass were higher at the Loam site (Fig 3e). In the buried soil at the Loam
435 site, $\Delta^{14}\text{C}$ values were higher in cores taken under the reference vegetation (Fig 3e). At the Clay
436 site, $\Delta^{14}\text{C}$ values within the top 30 cm were more depleted relative to the atmosphere than at the
437 other two sites (Fig 3f). The $\Delta^{14}\text{C}$ values declined steeply with depth at the Clay site, reaching
438 values in the -200 to -400 ‰ range at a depth of 1 m. At this site the $\Delta^{14}\text{C}$ depth profiles were
439 broadly similar under the two vegetation types (Fig 3f).

440



441
442 **Figure 3.** C isotopes versus depth. Data are from three replicate cores sampled under switchgrass
443 and paired “reference” annual crops at three sites in Oklahoma characterized by different soil
444 textures (Sandy Loam, panels a and d; Loam, panels b and e; Clay, panels c and f). Data from
445 each replicate core are shown individually. Cores taken under switchgrass are shown in blue, and
446 cores taken under the reference plot are shown in red. The soil at the Loam site featured a buried
447 profile, which is shown with a dashed gray line. The range of $\Delta^{14}\text{C}$ for the atmosphere over the
448 study period is shown as a gray region on the right of panels d-f. C isotope data could not be
449 collected at all depths at the Sandy Loam site because organic C concentrations were too low;
450 data gaps are interpolated with dashed lines.

451

452 3.6 Total organic C stocks

453 We obtained equivalent soil mass (ESM) estimates of C stocks at each site. The mean C
454 stocks for the top 500 kg m⁻² of soil (approximately 0-30 cm depth) and the lower 500-1500 kg
455 m⁻² of soil (approximately 30-100 cm depth) are reported in Table 3. While we focused on ESM
456 estimates when comparing plots to factor out bulk density differences between plots and sites,
457 we also report total estimates to a depth of 1.2 m—which was the greatest depth at which we
458 were able to collect samples across all sites—and to a depth of 2.4 m, which was attained at the
459 Sandy Loam and Loam sites (Table 3). All soil chemical data and C-isotope values are reported
460 in Supplementary Table 1.

461 We compared the C stocks under switchgrass and reference plots (Fig 4). At the Sandy
462 Loam site, direct comparison of the C stocks suggests that there was slightly more C under
463 switchgrass in the top 500 kg m⁻² of soil (stock difference = 0.4 kg C m⁻²; p < 0.01) and also in
464 the subsoil (stock difference = 1.5 kg C m⁻²; p < 0.01). At the Loam site, we observed
465 significantly more C under switchgrass in the top 500 kg m⁻² of soil (stock difference = 2.2 kg C
466 m⁻²; p < 0.01) and in the subsoil (stock difference = 0.6 kg C m⁻²; p = 0.01). At the Clay site, the
467 C stock difference in the top 500 kg m⁻² was comparatively small and not statistically significant
468 (stock difference = 0.2 kg C m⁻²; p = 0.4) and the same was true of the subsoil (stock difference
469 = 0.1 kg C m⁻²; p = 0.44).

470

Site	Plot	Organic C stock (kg m ⁻²)			
		0-500 kg m ⁻²	500-1500 kg m ⁻²	0-1.2 meter	0-2.4 meter
Clay	Switchgrass	3.9 (0.5)	2.7 (0.6)	7.4 (1.0)	n/a
	Reference	3.6 (0.8)	2.6 (0.2)	7.7 (1.1)	n/a
Sandy Loam	Switchgrass	1.7 (0.1)	2.7 (0.1)	5.7 (0.3)	7.3 (0.5)
	Reference	1.2 (0.1)	1.3 (0.1)	2.8 (0.3)	3.1 (0.3)
Loam	Switchgrass	4.7 (0.8)	2.8 (0.2)	8.9 (1.3)	13.3 (1.4)
	Reference	2.5 (0.1)	2.2 (0.1)	5.9 (0.3)	11.6 (0.5)

471

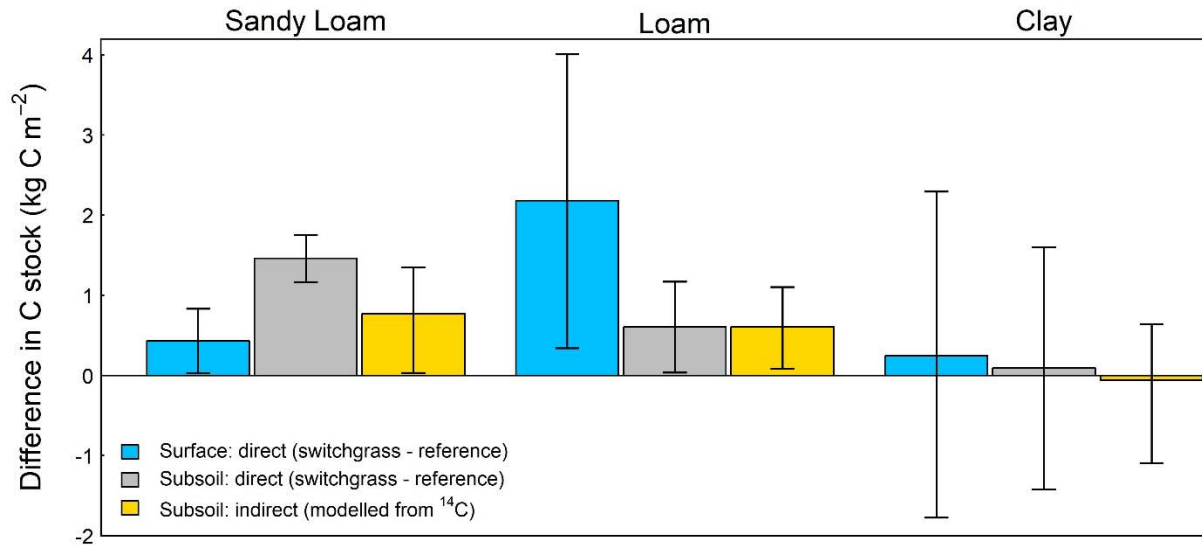
472 **Table 3. SOC stock estimates.** Data are from three replicate cores sampled under switchgrass
473 and paired “reference” annual crops at three sites in Oklahoma characterized by different soil
474 textures. Values are means, with standard deviations in parentheses. The first two columns of
475 data represent stocks estimated on an equivalent soil mass basis; the second two columns
476 represent stocks to a fixed depth. Stocks to 2.4 m are not shown for the Clay site because
477 sampling to this depth was not possible there, possibly due to calcium cementation in the subsoil.

478

479 3.7 Stock differences from ¹⁴C

480 Using the observed $\Delta^{14}\text{C}$ values, the observed C stocks under switchgrass, and equations 2-4,
481 we developed estimates of the difference in subsoil C stocks between the plots independently of
482 the reference plot C stock (Fig 4). Using Equation 3, we estimated that the fraction of additional
483 C introduced after switchgrass planting (f_n) was 0.31 at the Sandy Loam site, 0.21 at the Loam
484 site, and -0.01 (effectively zero) at the Clay site. By multiplying these values by the
485 corresponding C stocks in the switchgrass field we estimated that the ¹⁴C-based stock difference
486 at the Sandy Loam site was 0.84 kg C m⁻² ($p < 0.01$)—which was lower than the direct estimate
487 derived from subtracting the observed C stocks. At the Loam site, the ¹⁴C-based stock difference
488 was 0.6 kg C m⁻² ($p < 0.01$), which overlapped closely with the direct estimate. At the Clay site,
489 the ¹⁴C-based estimate was near zero and not statistically significant (-0.02 kg C m⁻²; $p = 0.48$).

490



491

492 **Figure 4.** Mean difference in C stock between the switchgrass and annual plant cover. Data are
493 from three replicate cores sampled under switchgrass and paired “reference” annual crops at
494 three sites in Oklahoma characterized by different soil textures. Blue bars show estimates for the
495 top 500 kg m⁻² of soil, gray bars show estimates for the lower 500-1500 kg m⁻² of soil, and
496 yellow bars show estimates for the lower 500-1500 kg m⁻² of soil based on the stock in the
497 switchgrass plot and the shift in $\Delta^{14}\text{C}$ between plots (Equations 2-4). Error bars show 95%
498 confidence intervals derived from Monte Carlo uncertainty propagation.

499

500 4. Discussion

501 4.1 Differences in SOC

502 At two out of the three sites we sampled, we observed significant differences in SOC
503 between switchgrass and reference plots in both topsoil (0-500 kg m⁻² soil mass, or
504 approximately 0-30 cm) and subsoil (500-1500 kg m⁻² soil mass, approximately 30-100 cm). At

505 these two sites, differences in subsoil C were in the range of 0.6-1.5 kg C m⁻². This range is
506 comparable to the value observed in subsoils at 42 paired sites where switchgrass was grown
507 across the upper Midwest (1.2 kg C m⁻²; Liebig et al, 2005). If these differences are normalized
508 by the time since planting at each site for the cumulative soil mass of 1500 kg m⁻²
509 (approximately 0-100 cm depth), the values are 1.9 Mg C ha⁻¹ y⁻¹ at the Sandy Loam site, 1.4 Mg
510 C ha⁻¹ y⁻¹ at the Loam site, and 0.3 Mg C ha⁻¹ y⁻¹ at the Clay site (direct stock comparison). If we
511 use ¹⁴C-based estimates for the subsoil rather than direct estimates, the time-normalized values
512 are similar: 1.24 Mg C ha⁻¹ y⁻¹ at the Sandy Loam site, 1.4 Mg C ha⁻¹ y⁻¹ at the Loam site, and
513 0.2 Mg C ha⁻¹ y⁻¹ at the Clay site. These values can be interpreted as “relative changes” in that
514 they estimate the (linear) rate of divergence between switchgrass and conventionally managed
515 systems. This range of rates is typical of switchgrass systems evaluated to a comparable depth
516 (Frank et al., 2004; Qin et al., 2016). Notably, divergence between the two land use types could
517 represent an unknown combination of C sequestration and avoided emissions, depending on the
518 absolute trajectory of C stocks in both fields (Sanderman and Baldock, 2010; Sanford et al.,
519 2012). The discrepancy makes the use of paired plots for C accounting purposes complicated—
520 but at the same time both negative emissions and avoided emissions would be benefits of
521 bioenergy crop production in marginal lands.

522 *4.2 Interpreting C isotopes*

523 Both ¹³C and ¹⁴C were sensitive to land use at the three sites, and in general ¹⁴C confirmed
524 that larger C stocks under switchgrass at these sites (or lack thereof) can be attributed to recently
525 fixed C in the subsoil. We did, however, discover some disagreement between the directly
526 measured C stocks and the difference estimated using ¹⁴C: the directly-measured difference in
527 subsoil C stocks was largest at the Sandy Loam, but the shift in ¹⁴C values at this site was too

528 small to fully accommodate this difference. The simplest interpretation of this result is that the
529 initial C stocks were greater under the switchgrass field before planting—highlighting the limits
530 of the small sample size ($n=3$) plus the spatially pseudo-replication inherent to the paired
531 sampling design. This interpretation is supported by texture analysis of deeper soil horizons at
532 this site: while soil properties in the upper 90 cm of the soil profile were similar in the reference
533 and switchgrass fields at this site, the reference plot had a higher profile-averaged sand to silt
534 ratio than switchgrass at depths exceeding 90 cm (mean sand/silt = 14 ± 0.7 versus 2 ± 0.4 at a
535 depth of 120 cm, Table S1). This indicates that soil physical characteristics did not match
536 perfectly at this site below a certain depth. At the other two sites where the plots were more
537 closely paired, direct and ^{14}C -based methods agreed.

538 Intriguingly, we observed less total C and comparatively depleted ^{14}C values in the buried
539 soil (paleosol) under switchgrass at the Loam site. The ^{14}C values in the paleosol were less
540 depleted under the reference plot—and were actually slightly less depleted than the overlying
541 soil (Fig 3e). Given that roots were not observable in the paleosol, we think it is unlikely that
542 patterns in total C and ^{14}C at the depth are driven by modern plant cover. Instead, we think it is
543 most likely that the soil under the switchgrass and reference plots—while similar now—
544 experienced different histories, resulting in different C stocks and isotopes at depth. The range of
545 ^{14}C values that we observed in the paleosol (-394 to -156 ‰) suggest that it was buried during
546 the mid- or late Holocene (i.e. in the last 5,000 years). It is possible that the paleosol under the
547 switchgrass plot was eroded prior to burial—which would explain its lower C concentrations and
548 ^{14}C values relative to the reference plot. The material that was subsequently deposited over both
549 paleosols may have been derived from upland soils containing ^{14}C -depleted organic matter,
550 which could explain why the upper part of the paleosol is richer in ^{14}C than the overlying base of
551 the modern soil (Lombardo et al., 2018). More generally, deep soil sampling in paired plots can

552 reveal inherited soil features that are not identifiable at the surface—particularly in the mid-
553 continental USA, where paleosols are common under alluvial and eolian deposits (Muhs, 2013).

554 We generally observed enrichment of ^{13}C under switchgrass, particularly at the Sandy Loam
555 site. C_4 plants like switchgrass have tissue $\delta^{13}\text{C}$ values ranging from -16 to -11 ‰, whereas C_3
556 plant tissue ranges from -30 to -20 ‰ (O’Leary, 1988). The shifts we observed are thus
557 consistent with an increase in the abundance of C_4 -derived C under switchgrass. Interpreting the
558 ^{13}C data quantitatively is challenging however, given that these sites have experienced a complex
559 history that has included a mix of C_3 and C_4 crops. The recent C_3 plant contribution may explain
560 ^{13}C depth profiles at the Sandy Loam and Loam sites, where $\delta^{13}\text{C}$ values in the top 30 cm of soil
561 were lower than those in the subsoil. However, the relatively higher $\delta^{13}\text{C}$ in the subsoil could
562 also reflect fractionation during decomposition (Menichetti et al., 2015; Werth and Kuzyakov,
563 2010). Given these complexities, it would be challenging to use ^{13}C as an unbiased tracer of
564 switchgrass C in the context of our sites—highlighting the value of ^{14}C .

565 *4.3 Explaining differences between sites*

566 The direct measurements of organic C and the isotopic calculations detected a similar trend:
567 there was more C under switchgrass at the Sandy Loam and Loam sites, and no difference
568 between switchgrass and reference plots at the Clay site. Multiple factors that might explain this
569 pattern given that the three sites have different soil properties and have also experienced different
570 management histories (e.g. tillage, and crop type in the reference fields). Furthermore, the
571 switchgrass stand at the Loam site was 10 years older than the stands at the other two sites.
572 Because these factors are correlated across sites, we have no way to identify which influenced
573 SOC most strongly. Regardless, the large apparent shift at the Sandy Loam site suggests that
574 management effects on C can be substantial even in coarse-textured soils.

575 **5. Conclusions**

576 We found that SOC stocks were significantly larger under switchgrass than in nearby reference
577 plots at two out of three sites in Oklahoma. SOC differences were significant at two sites with
578 coarse-textured soils, and not detectable at a site with fine-textured soils. By using ^{14}C as a tracer
579 of belowground inputs to the subsoil after planting we were able to confirm that differences in C
580 stocks at the three sites were at least partly attributable to recently fixed C under switchgrass.
581 This demonstrates that ^{14}C can be a useful tracer for divergence of SOC stocks following shifts
582 in cultivation or land use. Further application of ^{14}C via repeated measurements and analysis of
583 SOC fractions might help to constrain the trajectory of C stock dynamics, improving C
584 accounting following cultivation of perennial bioenergy crops.

585 **6. Acknowledgements**

586 This research is based upon work supported by the U.S. Department of Energy Office of Science,
587 awards SCW1555 and SCW1632 at Lawrence Livermore National Laboratory, award DE-
588 SC0014079 to UC Berkeley and a subcontract to the Noble Research Institute. Lawrence
589 Livermore National Laboratory's Lab Directed Research and Development program (#19-ERD-
590 010) contributed salary support for ES. Work at LLNL was conducted under the auspices of
591 DOE Contract DE-AC52- 07NA27344.

592 We thank Hugh Aljoe, Kelly Craven, James Rogers and Shawn Norton for facilitating site access
593 and soil collection at the Nobel Research Institute farms. We thank Yanqi Wu for the opportunity
594 to sample Oklahoma State University's field site near Stillwater, OK. Thanks also to Yuan
595 Wang, Na Ding, Travis Simmons, Josh Barbour, Mellisa McMahon, Jennifer Black, Konstantin
596 Chekhovskiy, Jialiang Kuang, Colin Bates, Ryan Gini, Noah Sokol and Ricardo Feliciano-Rivera
597 for their help with harvests and processing of soil samples.

598 **7. References**

- 599 Anderson-Teixeira, K.J., Davis, S.C., Masters, M.D., Delucia, E.H., 2009. Changes in soil
600 organic carbon under biofuel crops. *GCB Bioenergy* 1, 75–96. doi:10.1111/j.1757-
601 1707.2008.01001.x
- 602 Balesdent, J., Basile-Doelsch, I., Chadoeuf, J., Cornu, S., Derrien, D., Fekiacova, Z., Hatté, C.,
603 2018. Atmosphere–soil carbon transfer as a function of soil depth. *Nature* 559, 599–602.
604 doi:10.1038/s41586-018-0328-3
- 605 Balesdent, J., Mariotti, A., 1996. Measurement of turnover of soil organic matter using ¹³C
606 natural abundance, in: *Mass Spectrometry of Soils*. Marcel Dekker, New York.
- 607 Balesdent, J., Mariotti, A., Guillet, B., 1987. Natural ¹³C abundance as a tracer for studies of soil
608 organic matter dynamics. *Soil Biology and Biochemistry* 19, 25–30. doi:10.1016/0038-
609 0717(87)90120-9
- 610 Beniston, J.W., DuPont, S.T., Glover, J.D., Lal, R., Dungait, J.A.J., 2014. Soil organic carbon
611 dynamics 75 years after land-use change in perennial grassland and annual wheat
612 agricultural systems. *Biogeochemistry* 120, 37–49. doi:10.1007/s10533-014-9980-3
- 613 Brodie, C.R., Leng, M.J., Casford, J.S.L., Kendrick, C.P., Lloyd, J.M., Yongqiang, Z., Bird,
614 M.I., 2011. Evidence for bias in C and N concentrations and $\delta^{13}\text{C}$ composition of
615 terrestrial and aquatic organic materials due to pre-analysis acid preparation methods.
616 *Chemical Geology* 282, 67–83. doi:10.1016/j.chemgeo.2011.01.007
- 617 Burt, R., 2014. *Soil Survey Laboratory Methods Manual* (No 42. Version 5).
- 618 Conant, R.T., Cerri, C.E.P., Osborne, B.B., Paustian, K., 2017. Grassland management impacts
619 on soil carbon stocks: a new synthesis. *Ecological Applications* 27, 662–668.
620 doi:10.1002/eap.1473

- 621 Cotton, J.M., Cerling, T.E., Hoppe, K.A., Mosier, T.M., Still, C.J., 2016. Climate, CO₂, and the
622 history of North American grasses since the Last Glacial Maximum. *Science Advances* 2,
623 e1501346. doi:10.1126/sciadv.1501346
- 624 Davison, A.C., Hinkley, D.V., 1997. *Bootstrap methods and their application*. Cambridge
625 University Press.
- 626 Fisher, M.J., Rao, I.M., Ayarza, M.A., Lascano, C.E., Sanz, J.I., Thomas, R.J., Vera, R.R., 1994.
627 Carbon storage by introduced deep-rooted grasses in the South American savannas.
628 *Nature* 371, 236–238. doi:10.1038/371236a0
- 629 Frank, A.B., Berdahl, J.D., Hanson, J.D., Liebig, M.A., Johnson, H.A., 2004. Biomass and
630 Carbon Partitioning in Switchgrass. *Crop Science* 44, 1391–1396.
631 doi:10.2135/cropsci2004.1391
- 632 Garten, C.T., Wullschlegel, S.D., 2000. Soil Carbon Dynamics beneath Switchgrass as Indicated
633 by Stable Isotope Analysis. *Journal of Environmental Quality* 29, 645–653.
634 doi:10.2134/jeq2000.00472425002900020036x
- 635 Gelfand, I., Sahajpal, R., Zhang, X., Izaurralde, R.C., Gross, K.L., Robertson, G.P., 2013.
636 Sustainable bioenergy production from marginal lands in the US Midwest. *Nature* 493,
637 514–517. doi:10.1038/nature11811
- 638 Gifford, R.M., Roderick, M.L., 2003. Soil carbon stocks and bulk density: spatial or cumulative
639 mass coordinates as a basis of expression? *Global Change Biology* 9, 1507–1514.
640 doi:10.1046/j.1365-2486.2003.00677.x
- 641 Grayston, S.J., Vaughan, D., Jones, D., 1997. Rhizosphere carbon flow in trees, in comparison
642 with annual plants: the importance of root exudation and its impact on microbial activity
643 and nutrient availability. *Applied Soil Ecology* 5, 29–56. doi:10.1016/S0929-
644 1393(96)00126-6

- 645 Harris, Z.M., Spake, R., Taylor, G., 2015. Land use change to bioenergy: A meta-analysis of soil
646 carbon and GHG emissions. *Biomass and Bioenergy* 82, 27–39.
647 doi:10.1016/j.biombioe.2015.05.008
- 648 Harrison, R.B., Footen, P.W., Strahm, B.D., 2010. Deep Soil Horizons: Contribution and
649 Importance to Soil Carbon Pools and in Assessing Whole-Ecosystem Response to
650 Management and Global Change. *Forest Science* 57, 67–76.
- 651 Hua, Q., Barbetti, M., Rakowski, A.Z., 2013. Atmospheric Radiocarbon for the Period 1950–
652 2010. *Radiocarbon* 55, 2059–2072. doi:10.2458/azu_js_rc.v55i2.16177
- 653 Huang, H., 2019. Why the scaled and shifted t-distribution should not be used in the Monte Carlo
654 method for estimating measurement uncertainty? *Measurement* 136, 282–288.
655 doi:10.1016/j.measurement.2018.12.089
- 656 Jobbágy, E.G., Jackson, R.B., 2000. The vertical distribution of soil organic carbon and its
657 relation to climate and vegetation. *Ecological Applications* 10, 423–436.
658 doi:[https://doi.org/10.1890/1051-0761\(2000\)010\[0423:TVDOSO\]2.0.CO;2](https://doi.org/10.1890/1051-0761(2000)010[0423:TVDOSO]2.0.CO;2)
- 659 Jones, M.B., Donnelly, A., 2004. Carbon sequestration in temperate grassland ecosystems and
660 the influence of management, climate and elevated CO₂: Tansley review. *New*
661 *Phytologist* 164, 423–439. doi:10.1111/j.1469-8137.2004.01201.x
- 662 Kell, D.B., 2012. Large-scale sequestration of atmospheric carbon via plant roots in natural and
663 agricultural ecosystems: why and how. *Philosophical Transactions of the Royal Society*
664 *B: Biological Sciences* 367, 1589–1597. doi:10.1098/rstb.2011.0244
- 665 Komada, T., Anderson, M.R., Dorfmeier, C.L., 2008. Carbonate removal from coastal sediments
666 for the determination of organic carbon and its isotopic signatures, $\delta^{13}\text{C}$ and $\Delta^{14}\text{C}$:
667 comparison of fumigation and direct acidification by hydrochloric acid: Carbonate

- 668 removal from coastal sediments. *Limnology and Oceanography: Methods* 6, 254–262.
669 doi:10.4319/lom.2008.6.254
- 670 Kravchenko, A.N., Robertson, G.P., 2011. Whole-Profile Soil Carbon Stocks: The Danger of
671 Assuming Too Much from Analyses of Too Little. *Soil Science Society of America*
672 *Journal* 75, 235–240. doi:10.2136/sssaj2010.0076
- 673 Ledo, A., Smith, P., Zerihun, A., Whitaker, J., Vicente □ Vicente, J.L., Qin, Z., McNamara, N.P.,
674 Zinn, Y.L., Llorente, M., Liebig, M., Kuhnert, M., Dondini, M., Don, A., Diaz □ Pines, E.,
675 Datta, A., Bakka, H., Aguilera, E., Hillier, J., 2020. Changes in soil organic carbon under
676 perennial crops. *Global Change Biology* gcb.15120. doi:10.1111/gcb.15120
- 677 Lemus, R., Lal, R., 2005. Bioenergy Crops and Carbon Sequestration. *Critical Reviews in Plant*
678 *Sciences* 24, 1–21. doi:10.1080/07352680590910393
- 679 Liebig, M.A., Johnson, H.A., Hanson, J.D., Frank, A.B., 2005. Soil carbon under switchgrass
680 stands and cultivated cropland. *Biomass and Bioenergy* 28, 347–354.
681 doi:10.1016/j.biombioe.2004.11.004
- 682 Liebig, M.A., Schmer, M.R., Vogel, K.P., Mitchell, R.B., 2008. Soil Carbon Storage by
683 Switchgrass Grown for Bioenergy. *BioEnergy Research* 1, 215–222. doi:10.1007/s12155-
684 008-9019-5
- 685 Lombardo, U., Rodrigues, L., Veit, H., 2018. Alluvial plain dynamics and human occupation in
686 SW Amazonia during the Holocene: A paleosol-based reconstruction. *Quaternary*
687 *Science Reviews* 180, 30–41. doi:10.1016/j.quascirev.2017.11.026
- 688 Lorenz, K., Lal, R., 2005. The Depth Distribution of Soil Organic Carbon in Relation to Land
689 Use and Management and the Potential of Carbon Sequestration in Subsoil Horizons, in:
690 *Advances in Agronomy*. Elsevier, pp. 35–66. doi:10.1016/S0065-2113(05)88002-2

- 691 Lynch, J.P., Wojciechowski, T., 2015. Opportunities and challenges in the subsoil: pathways to
692 deeper rooted crops. *Journal of Experimental Botany* 66, 2199–2210.
693 doi:10.1093/jxb/eru508
- 694 Marin-Spiotta, E., Silver, W.L., Swanston, C.W., Ostertag, R., 2009. Soil organic matter
695 dynamics during 80 years of reforestation of tropical pastures. *Global Change Biology*
696 15, 1584–1597. doi:10.1111/j.1365-2486.2008.01805.x
- 697 Mathieu, J.A., Hatté, C., Balesdent, J., Parent, É., 2015. Deep soil carbon dynamics are driven
698 more by soil type than by climate: a worldwide meta-analysis of radiocarbon profiles.
699 *Global Change Biology* 21, 4278–4292. doi:10.1111/gcb.13012
- 700 Menichetti, L., Houot, S., van Oort, F., Kätterer, T., Christensen, B.T., Chenu, C., Barré, P.,
701 Vasilyeva, N.A., Ekblad, A., 2015. Increase in soil stable carbon isotope ratio relates to
702 loss of organic carbon: results from five long-term bare fallow experiments. *Oecologia*
703 177, 811–821. doi:10.1007/s00442-014-3114-4
- 704 Minasny, B., Malone, B.P., McBratney, A.B., Angers, D.A., Arrouays, D., Chambers, A.,
705 Chaplot, V., Chen, Z.-S., Cheng, K., Das, B.S., Field, D.J., Gimona, A., Hedley, C.B.,
706 Hong, S.Y., Mandal, B., Marchant, B.P., Martin, M., McConkey, B.G., Mulder, V.L.,
707 O'Rourke, S., Richer-de-Forges, A.C., Odeh, I., Padarian, J., Paustian, K., Pan, G.,
708 Poggio, L., Savin, I., Stolbovoy, V., Stockmann, U., Sulaeman, Y., Tsui, C.-C., Vågen,
709 T.-G., van Wesemael, B., Winowiecki, L., 2017. Soil carbon 4 per mille. *Geoderma* 292,
710 59–86. doi:10.1016/j.geoderma.2017.01.002
- 711 Monti, A., Barbanti, L., Zatta, A., Zegada-Lizarazu, W., 2012. The contribution of switchgrass in
712 reducing GHG emissions. *GCB Bioenergy* 4, 420–434. doi:10.1111/j.1757-
713 1707.2011.01142.x

- 714 Muhs, D.R., 2013. 11.9 Loess and its Geomorphic, Stratigraphic, and Paleoclimatic Significance
715 in the Quaternary, in: *Treatise on Geomorphology*. Elsevier, pp. 149–183.
716 doi:10.1016/B978-0-12-374739-6.00302-X
- 717 National Cooperative Soil Survey, 2020. National Cooperative Soil Characterization Database.
- 718 O’Brien, S.L., Jastrow, J.D., McFarlane, K.J., Guilderson, T.P., Gonzalez-Meler, M.A., 2013.
719 Decadal cycling within long-lived carbon pools revealed by dual isotopic analysis of
720 mineral-associated soil organic matter. *Biogeochemistry* 112, 111–125.
721 doi:10.1007/s10533-011-9673-0
- 722 O’Leary, M.H., 1988. Carbon Isotopes in Photosynthesis. *BioScience* 38, 328–336.
723 doi:10.2307/1310735
- 724 Parfitt, R.L., Ross, C., Schipper, L.A., Claydon, J.J., Baisden, W.T., Arnold, G., 2010.
725 Correcting bulk density measurements made with driving hammer equipment. *Geoderma*
726 157, 46–50. doi:10.1016/j.geoderma.2010.03.014
- 727 Paulsen, G.M., Shroyer, J.P., 2008. The Early History of Wheat Improvement in the Great
728 Plains. *Agronomy Journal* 100, S-70-S-78. doi:10.2134/agronj2006.0355c
- 729 Paustian, K., Lehmann, J., Ogle, S., Reay, D., Robertson, G.P., Smith, P., 2016. Climate-smart
730 soils. *Nature* 532, 49–57. doi:10.1038/nature17174
- 731 Pribyl, D.W., 2010. A critical review of the conventional SOC to SOM conversion factor.
732 *Geoderma* 156, 75–83. doi:10.1016/j.geoderma.2010.02.003
- 733 Qin, Z., Dunn, J.B., Kwon, H., Mueller, S., Wander, M.M., 2016. Soil carbon sequestration and
734 land use change associated with biofuel production: empirical evidence. *GCB Bioenergy*
735 8, 66–80. doi:10.1111/gcbb.12237
- 736 Rasse, D.P., Rumpel, C., Dignac, M.-F., 2005. Is soil carbon mostly root carbon? Mechanisms
737 for a specific stabilisation. *Plant and Soil* 269, 341–356. doi:10.1007/s11104-004-0907-y

- 738 Richter, D.D., Markewitz, D., Trumbore, S.E., Wells, C.G., 1999. Rapid accumulation and
739 turnover of soil carbon in a re-establishing forest. *Nature* 400, 56–58. doi:10.1038/21867
- 740 Robertson, G.P. (Ed.), 1999. Standard soil methods for long-term ecological research, Long-term
741 ecological research network series. Oxford University Press, New York.
- 742 Robertson, G.P., Hamilton, S.K., Barham, B.L., Dale, B.E., Izaurralde, R.C., Jackson, R.D.,
743 Landis, D.A., Swinton, S.M., Thelen, K.D., Tiedje, J.M., 2017. Cellulosic biofuel
744 contributions to a sustainable energy future: Choices and outcomes. *Science* 356,
745 eaal2324. doi:10.1126/science.aal2324
- 746 Rovira, P., Sauras, T., Salgado, J., Merino, A., 2015. Towards sound comparisons of soil carbon
747 stocks: A proposal based on the cumulative coordinates approach. *CATENA* 133, 420–
748 431. doi:10.1016/j.catena.2015.05.020
- 749 Rumpel, C., Kögel-Knabner, I., 2011. Deep soil organic matter—a key but poorly understood
750 component of terrestrial C cycle. *Plant and Soil* 338, 143–158. doi:10.1007/s11104-010-
751 0391-5
- 752 Sanderman, J., Baldock, J.A., 2010. Accounting for soil carbon sequestration in national
753 inventories: a soil scientist’s perspective. *Environmental Research Letters* 5, 034003.
754 doi:10.1088/1748-9326/5/3/034003
- 755 Sanderman, J., Hengl, T., Fiske, G.J., 2017. Soil carbon debt of 12,000 years of human land use
756 7.
- 757 Sanford, G.R., Posner, J.L., Jackson, R.D., Kucharik, C.J., Hedtcke, J.L., Lin, T.-L., 2012. Soil
758 carbon lost from Mollisols of the North Central U.S.A. with 20 years of agricultural best
759 management practices. *Agriculture, Ecosystems & Environment* 162, 68–76.
760 doi:10.1016/j.agee.2012.08.011

- 761 Sher, Y., Baker, N.R., Herman, D., Fossum, C., Hale, L., Zhang, X., Nuccio, E., Saha, M., Zhou,
762 J., Pett-Ridge, J., Firestone, M., 2020. Microbial extracellular polysaccharide production
763 and aggregate stability controlled by switchgrass (*Panicum virgatum*) root biomass and
764 soil water potential. *Soil Biology and Biochemistry* 143, 107742.
765 doi:10.1016/j.soilbio.2020.107742
- 766 Sierra, C.A., Müller, M., Trumbore, S.E., 2012. Models of soil organic matter decomposition:
767 the SoilR package, version 1.0. *Geoscientific Model Development* 5, 1045–1060.
768 doi:10.5194/gmd-5-1045-2012
- 769 Sokol, N.W., Kuebbing, Sara.E., Karlsen-Ayala, E., Bradford, M.A., 2019. Evidence for the
770 primacy of living root inputs, not root or shoot litter, in forming soil organic carbon. *New*
771 *Phytologist* 221, 233–246. doi:10.1111/nph.15361
- 772 Stuiver, M., Polach, H.A., 1977. Discussion Reporting of ¹⁴C Data. *Radiocarbon* 19, 355–363.
773 doi:10.1017/S0033822200003672
- 774 Syswerda, S.P., Corbin, A.T., Mokma, D.L., Kravchenko, A.N., Robertson, G.P., 2011.
775 Agricultural Management and Soil Carbon Storage in Surface vs. Deep Layers. *Soil*
776 *Science Society of America Journal* 75, 92–101. doi:10.2136/sssaj2009.0414
- 777 Trumbore, S., 2009. Radiocarbon and Soil Carbon Dynamics. *Annual Review of Earth and*
778 *Planetary Sciences* 37, 47–66. doi:10.1146/annurev.earth.36.031207.124300
- 779 Vogel, J.S., Southon, J.R., Nelson, D.E., Brown, T.A., 1984. Performance of catalytically
780 condensed carbon for use in accelerator mass spectrometry. *Nuclear Instruments and*
781 *Methods in Physics Research Section B: Beam Interactions with Materials and Atoms* 5,
782 289–293. doi:10.1016/0168-583X(84)90529-9

- 783 Wendt, J.W., Hauser, S., 2013. An equivalent soil mass procedure for monitoring soil organic
784 carbon in multiple soil layers. *European Journal of Soil Science* 64, 58–65.
785 doi:10.1111/ejss.12002
- 786 Werth, M., Kuzyakov, Y., 2010. ¹³C fractionation at the root–microorganisms–soil interface: A
787 review and outlook for partitioning studies. *Soil Biology and Biochemistry* 42, 1372–
788 1384. doi:10.1016/j.soilbio.2010.04.009
- 789